Characterization of a GH2/GO2 Combustor for Hot Plume Wind Tunnel Testing

By D. Kirchheck AND A. Gülhan

German Aerospace Center (DLR), Institute of Aerodynamics and Flow Technology
Supersonic and Hypersonic Technology Department
Linder Höhe, 51147 Cologne, Germany

After entry into operations of the newly implemented GH2/GO2 supply facility for hot plume testing at the German Aerospace Center (DLR), Cologne, facility operation in combination with the preliminary GH2/GO2 rocket combustion chamber is being characterized in order to qualify the test environment for future wind tunnel tests. The combustion chamber will be implemented into a generic rocket model to generate a realistic hot exhaust jet for interaction experiments with the transonic ambient flow, provided by the Vertical Test Section Cologne (VMK). Two reference configurations, that will be subject to investigation within the wind tunnel campaign, are characterized in the present paper by the facility operating parameters, combustion chamber pressure, and wall temperature distribution. An evaluation of the pressure fluctuation amplitudes, together with spectral analyzes is used for a classification of the state of combustion. The result is a summary of the different test cases with a discussion of their qualification for wind tunnel testing and an outlook on possible measures to extend the operating range for an enhanced range of similarity parameters.

1. Introduction

1.1. *Motivation for Hot Plume Wind Tunnel Testing*

The investigation of base flow phenomena on current and future space transportation vehicles with focus on the interaction of the ambient flow and the exhaust jet flow is a core research area of the *Collaborative Research Centre* (SFB) *Transregio 40* (TRR40) [1, 2]. Previous publications indicate, that the buffet phenomenon, known to be the reason for prominent launcher failures (e. g. the Ariane 5 flight 157), is closely linked to the interaction flow field, especially for long nozzle structures with a length of more than one base diameter [3, 4].

Nevertheless, until now, previous investigations are limited to cold-cold-interaction where the exhaust is modeled experimentally or numerically using moderately heated air or helium [5–7]. Since the flow-flow-interaction is assumed to be significantly influenced by the dynamics of their inherent shear flow development, the relative flow velocity between the ambient and exhaust stream could be one of the most important influence factors for the combined wake flow characteristics.

To investigate this influence on the resulting mechanical and thermal loads on the base and nozzle structure and evaluate the cold gas simulation technique for aerodynamics investigations, an approach of enhanced similarity by using hot gas simulation

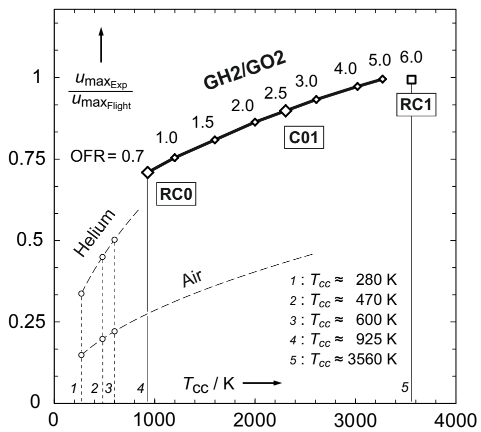

FIGURE 1. Similarity of the maximum nozzle exit velocity for different propulsive media depending one the total chamber temperature

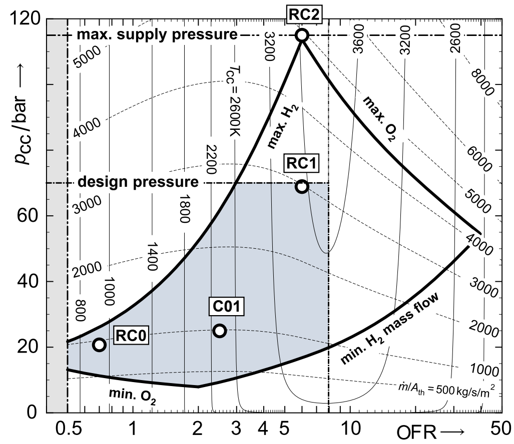

FIGURE 2. Operating range of the GH2/GO2 supply facility in combination with the current design of the test combustor

with more realistic stagnation conditions and more realistic exhaust jet properties is followed in the present work.

1.2. *Objectives of Future Wind Tunnel Tests*

In future wind tunnel tests, the exhaust jet will be generated by the combustion of gaseous oxygen and hydrogen (GH2/GO2) within an integrated combustion chamber inside the wind tunnel model. The resulting potential for an enhancement of the similarity with respect to stagnation conditions and gas properties is pictured in Fig. 1 as the ratio of the maximum vacuum nozzle exit velocity between experiment and flight. In this case, Ariane 5 is taken as the flight reference for similarity considerations.

The tests will be conducted around different reference configurations, mainly defined by the total mass flow rate $\dot{m}$ and the oxidizer to fuel mass flow ratio $\mathrm{OFR} = \dot{m}_{\mathrm{O2}}/\dot{m}_{\mathrm{H2}}$, labeled in Fig. 1 and 2 as RC0, RC1, and C01. The configurations RC0 and RC1 will enclose the targeted operating range. For RC0, mechanical and thermal loads on the test model are relatively low, which enables a higher level of instrumentation and more detailed comparisons with parallel numerical investigations. The configuration RC1 will result in an excellent similarity of the velocity ratio, but this introduces very challenging model design and operation requirements. As a compromise, condition C01 is designed to provide sufficiently realistic stagnation conditions, while limiting the complexity to an affordable level.

1.3. *Test Combustor*

Prior to performing wind tunnel tests, a characterization of the new GH2/GO2 supply facility [8, 9], covering the targeted range of future operating conditions is needed (see Fig. 2). For that, a robust and flexible preliminary test combustor was introduced [10,11]. Its modular design enables the qualification of materials and operating principles for a sophisticated development of the wind tunnel model including the combustion chamber. After entry into facility operation [11], the present work deals with preliminary tests at the targeted reference conditions to validate the chamber and injector concept for further aerodynamic and aerothermal investigations with the final wind tunnel model.

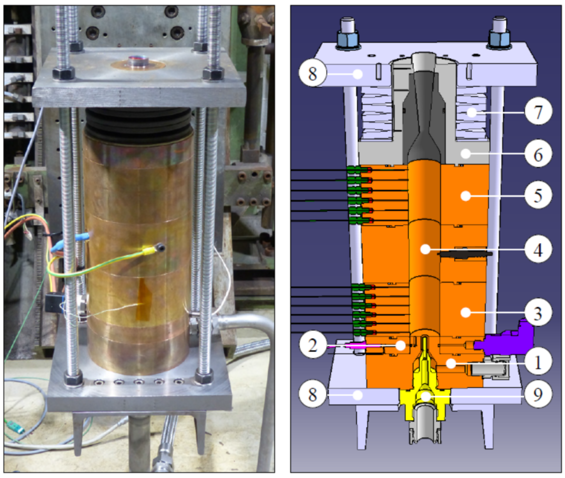

FIGURE 3. Photograph and 3D sectional view of the test combustor: 1 - injector body, 2 - pressure port, 3 - chamber temperature measurement module, 4 - ignition module, 6 - nozzle module, 9 - coaxial injector element

2. Experimental Methods

2.1. *Test Environment*

The test combustor for static combustion tests without ambient flow was integrated into the test chamber of the *Vertical Test Section Cologne* (VMK). The VMK is a blow down type wind tunnel with an open vertical free stream test section. Maximum reservoir conditions of 35 bar and 750 K enable a Mach number range from subsonic to supersonic conditions up to Mach 3.0 using several discrete nozzles.

For the GH2/GO2 supply, gaseous oxygen and hydrogen is stored in bundle stations at 300 bar storage pressure. At the control station, a pressure controller sets a constant reservoir pressure of 130 bar for the closed-loop mass flow controller. The maximum design condition (RC2) corresponds to oxygen and hydrogen mass flow rates of $\dot{m}_{O2} = 397.4$ g/s and $\dot{m}_{H2} = 66.4$ g/s at 115 bar.

2.2. *Test Model*

The test model is a stand-alone combustor, see Fig. 3, which is derived from the well-known *Penn State Design*. This approach allows taking advantage of published knowledge and opens up a range of comparative studies [12]. The design uses a modular design, where the chamber modules, equipped with either temperature sensors, pressure sensors or a spark ignitor can be arranged in different order. The injector is a single element coaxial shear injector, which is replaceable to allow for easy modifications of the injectors geometry. At the nozzle part, the module can be equipped with either a copper or molybdenum module. The molybdenum module uses a replaceable graphite inlay to prevent the nozzle throat from erosion or fatal oxidation.

2.3. *Measurements and Instrumentation*

The combustor is equipped with a high frequency pressure transducer (Kulite XTEH-7L-190LM) at the base plate of the combustion chamber at a radius of 12.5 mm next to the injector post. In the vicinity of the pressure sensor head, a type K thermocouple is located to monitor the temperature impact. For measuring the temperature distribution

	run#	$\overline{\dot{m}}$ / (g/s)	$\overline{\text{OFR}}$	injector	nozzle	scope
baseline (RC0)	V137	89.16	0.70	I02	N56	suitability for wind tunnel testing, repeatability
	V139	89.16	0.70	I02	N56	
	V141	89.16	0.70	I02	N56	
OFR variation	V128	89.16	0.70	I02	N56	stability, injector off-design performance, material qualification
	V129	84.27	1.00	I02	N56	
	V130	80.25	1.50	I02	N56	
	V131	78.56	2.00	I02	N56	
	V132	77.95	2.50	I02	N56	
pressure variation[a]	V100	92.79	0.72	I02	N56	stability, injector off-design performance, material qualification
	V101	154.22	1.95	I02	N56	
	V102	198.97	2.23	I02	N56	
	V104	233.14	3.01	I02	N56	
	V105	309.84	2.98	I02	N56	
injector variation (C01)	V132	77.95	2.50	I02	N56	sensitivity to injector design
	V145	77.95	2.50	I02	N56	
	V134	77.95	2.50	I04	N56	
	V143	77.95	2.50	I04	N56	

[a] Values for V100 to V105 are given as measured values.

TABLE 1. Test program

inside the combustion chamber, thermocouples are flush-mounted to the inner chamber wall with direct contact to the combustion gases. They are equally spaced along the axial direction of the chamber with an axial distance of $\Delta x = 12.5\,\text{mm}$, starting at $x_1 = 6.25\,\text{mm}$ from the chamber base plate. For additional health monitoring, some tests include further temperature measurements inside the structure around the nozzle throat and exit plane. As input conditions, static pressures and temperatures, as well as mass flow rates of oxygen and hydrogen are measured upstream in the supply lines. The plume structure is made visible by *High-Speed Schlieren Videography* (HSS), which is automatically triggered by the data acquisition system.

2.4. *Test Program*

The present tests were designed to characterize the control algorithms, and accuracy of the supply system, as well as the output of the combustor. Since it will be one of the major input parameters for the future interaction experiments, focus is on the reference configuration RC0 and the development of the combustors range of operation towards higher conditions with more realistic stagnation and jet properties. A summary of the evaluated test cases with the main set point values is given in Tab. 1.†

Next to the baseline test cases at RC0 (V137 to V141), a variation of the oxidizer–fuel–ratio at approximately constant chamber pressure was performed. This was done in order to investigate higher temperature operation with respect to materials qualification and suitability of the injector concept at off-design conditions, including stability consid-

† Set point values are labeled with an overline $\overline{\xi}$, measured values are plain variables ξ.

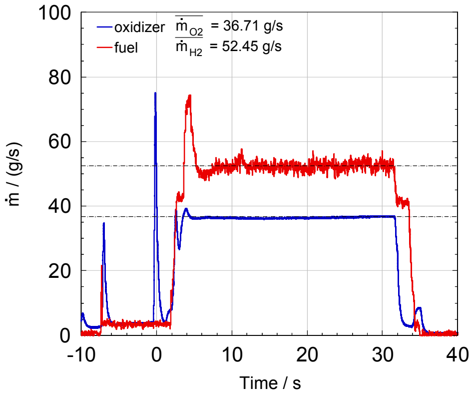

FIGURE 4. Oxidizer and fuel mass flow rates during a 30 s run at RC0 (V139); —-— set point values

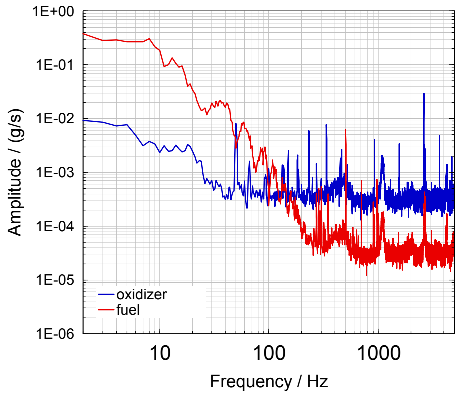

FIGURE 5. Spectogramm of the oxidizer and fuel mass flow signals between 25 and 30 s at RC0 (V139)

erations (V128 to V132). In addition to that, an increase of the mass flow rate, hence, chamber pressure was also investigated for the same reasons (V100 to V105). Finally, further tests with geometric modifications of the injectors exit cross sections provides insight into the sensitivity of the test setup to the injector design (V132, V145, V134, V143).

3. Results

3.1. *Operating Conditions at RC0*

Figure 4 shows the actively controlled oxidizer and fuel mass flows for an exemplary run at reference condition RC0 (V139). The total run duration is 30 s inlcuding ramping the set point curve at the beginning of the run from 0 to 2 s in an open control loop and then activating the closed-loop control for the nominal mass flow rate. At the end of the run, the oxygen mass flow is cut 2 s before the hydrogen for cooling reasons and to avoid oxygen-rich mixtures within the cut-off transient. The mass flow controller reached nominal and constant conditions at approximately 6 s into the run for oxygen and 7 s for hydrogen. This gives an average valid test duration of 23 s. For a more detailed description on the ignition and start-up process refer to [11].

The spectral content of the mass flow signals is given in Fig. 5, aiming at localizing low-frequency spectral characteristics of the piping, mass flow controller, or control valves. In the frequency domain, the fluctuating mass flow signals are represented by uniformly distributed low-frequency broad band spectra without significant maxima. These spectra extend to 50 Hz for the oxidizer mass flow and 200 Hz for the fuel mass flow. The content of the higher spectrum is beyond the sensors natural frequencies and approximately one to four orders of magnitude lower than the flow signal, which offers a good signal to noise ratio and does not contribute significantly to the sequences in Fig. 4. Therefore, we interpret the mass flow signals as representations of randomly occurring flow fluctuations without predominant oscillatory disturbances from the control path including the sensor and without predominant oscillatory disturbances from historical flow events in the resolved frequency range.

The accuracy of the inflow to the combustion chamber is shown in Fig. 6 with respect to the set point values within the last 5 s of the nominal run time. Primary input

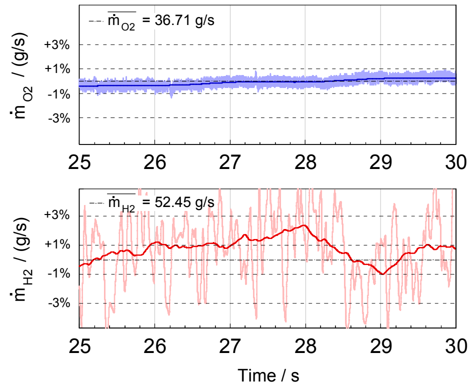

FIGURE 6. Accuracy of the mass flow signals w. r. t. the set point values at RC0 (V139)

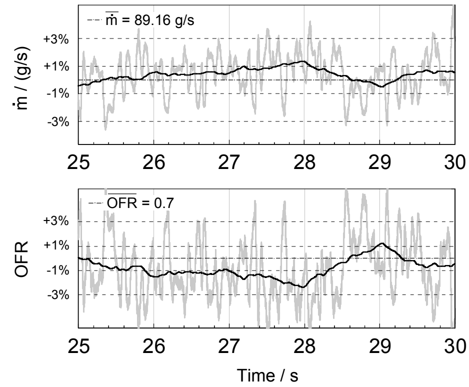

FIGURE 7. Accuracy of the total mass flow rate and oxidizer–fuel–ratio at RC0 (V139)

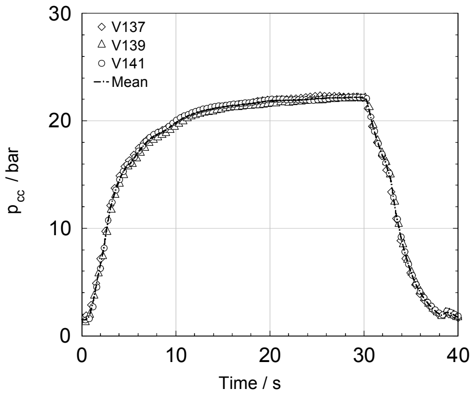

FIGURE 8. Repeatability of the total chamber pressure for a 30 s run at RC0 (V137, V139, V141)

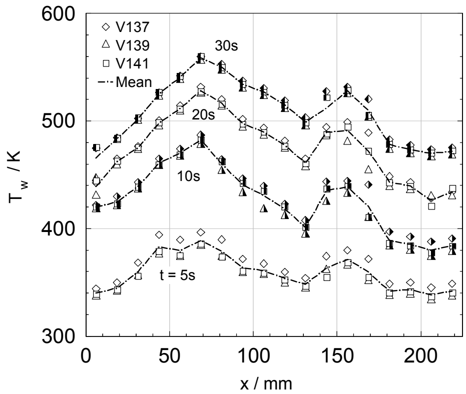

FIGURE 9. Repeatability of the wall temperature distribution after 5, 10, 20, and 30 s at RC0 (V137, V139, V141)

parameters are the oxidizer and hydrogen mass flows $\dot{m}_{O2}$ and $\dot{m}_{H2}$. Secondary input parameters are the total mass flow rate $\dot{m}$ and the oxidizer–fuel–ratio OFR, which are calculated from the individual flow signals. The signals were filtered by a running mean with an interval time of 500 ms to isolate the controlled mean stream. The oxidizer mass flow was kept within a $\pm1\%$ error interval. The hydrogen mass flow is within the $\pm3\%$ range, whereas the the relative root-mean-square (RMS) of the raw signal $\dot{m}_{H2}^{RMS}$ is within $\pm2.5\%$. The accuracy of the total mass flow and the oxidizer–fuel–ratio is mainly driven by the hydrogen mass flow signal. The respective signals are given in Fig. 7 for convenience.

The resulting chamber conditions are pictured in Fig. 8 and Fig. 9 as the total chamber pressure p_{cc} and the chamber wall temperature profile T_w along the axial direction at different instances of time. Each graph comprises the measurements from three individual test runs at RC0, together with their resulting average. An evaluation of the chamber pressure at 5, 10, 20, and 30 s run time leads to a relative standard deviation of 1.3% to 0.2% respectively, meaning that not only the final constant condition, but also the transient process are well repeatable. The range of the maximum to minimum pressure

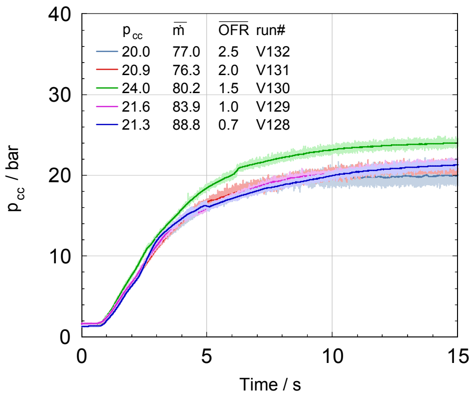

FIGURE 10. Chamber pressures for different oxidizer–fuel–ratios

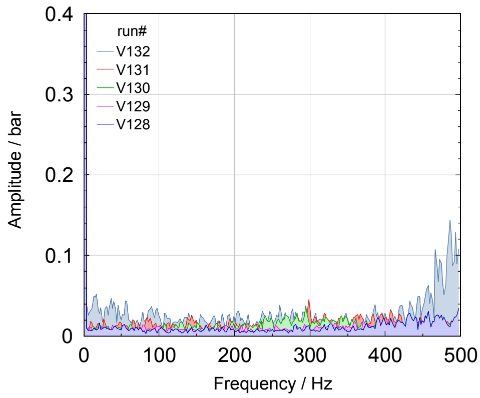

FIGURE 11. Spectral analysis of the pressure signals from Fig. 10 at different mass flow rates and oxidizer–fuel–ratios

inside the evaluation interval $p'^{\text{p-p}}_{\text{cc}}$ is averaged to 1.75 bar for the RC0 test cases (V137, V139, V141), which is $\pm$3.9% relative to the mean pressure. According to [13], this state it is called *smooth combustion*, since the relative peak-to-peak amplitude $p'^{\text{p-p}}_{\text{cc}}/2p_{\text{cc}}$ is less than $\pm$5%.

The wall temperatures are evaluated at 5, 10, 20, and 30 s as profiles in the axial direction. After the mass flow is fully established at $t \approx 7$ s, the profiles are qualitatively independent from run time. Repeatability is again proven by multiple runs with minor deviations, especially after long run times. In the axial direction, the temperature rises up to $x_6 \approx 70$ mm behind the chamber base, where the maximum temperature is located. A second peak is located at $x_{13} \approx 156$ mm, before the temperature falls down to the minimum value at $x_{17} \approx 200$ mm. The first peak is in accordance with the attachment of the core flow at the wall [10, 12]. The surrounded annular recirculation region grows with increasing mass flow within the start-up transient and keeps a constant length after reaching nominal conditions. The second peak is not reported in literature and was not observed in CFD calculations. Compared to literature, the oxidizer–fuel–ratio is significantly higher in the present test case and compared to the 2D-axisymmetric CFD calculation, the hydrogen inflow is strongly non-axisymmetric, due to a 90° elbow shortly upstream of the injector. Finally, unexpectedly high wall temperatures or heat fluxes might be an indicator for instabilities, according to the description in [14] (refer to Sec. 4 for more information).

3.2. *Variation of the Oxidizer–Fuel–Ratio*

Several tests were carried out in order to investigate combustion roughness and low frequency stability, related to the propellant feed system (V128 to V132). A variation of the oxidizer–fuel–ratio was performed at constant injector geometry between ratios of 0.7 to 2.5. Therefore, injection velocities change with OFR. The development of the chamber pressures is pictured in Fig. 10 as running mean and as raw signals. The mass flow rates were adapted in these tests to reach approximately 21 bar for comparability reasons. The relative fluctuation amplitude increases with OFR from $\pm$3.1% to $\pm$8.9%. Cases with OFR $\leq$ 1.5 showed smooth combustion. For OFR $>$ 2.0, combustion becomes rough. The characteristics, evaluated at 15 s are given in Tab. 2.

For these tests, no clear difference is visible for the spectral distribution within a 500 Hz

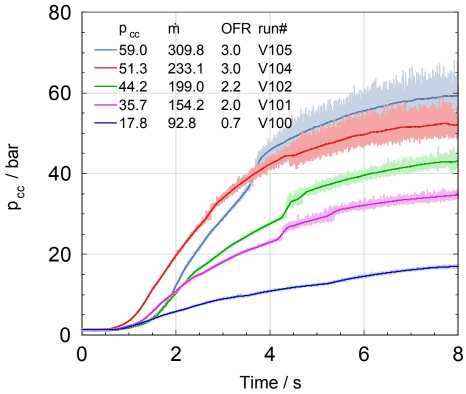

FIGURE 12. Chamber pressures for different mass flow rates and oxidizer–fuel–ratios

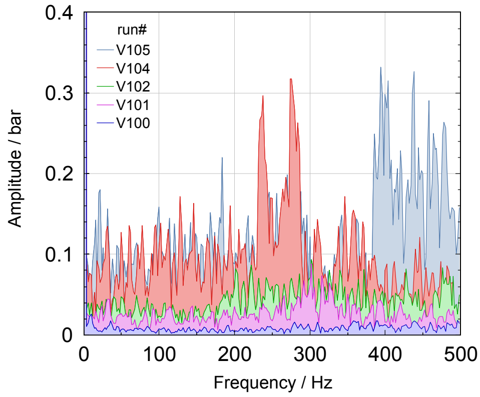

FIGURE 13. Spectral analysis of the pressure signals from Fig. 12 at different mass flow rates and oxidizer–fuel–ratios

range (Fig. 11). Apparently, the determining band is shifted from approximately 200 Hz (V129) over 270 Hz (V130), 350 Hz (V131) to 480 Hz (V132) with increasing OFR and increasing chamber temperature. But, for the lower conditions the elevation relative to the surrounding spectrum is not sufficient for drwaing conclusions.

3.3. *Variation of the Total Mass Flow*

Similar tests were carried out with a focus on the variation of the total mass flow rate, given in Fig. 12 and Fig. 13. The total mass flow ranges from approximately 93 to 310 g/s at about 21 to 60 bar chamber pressure. The oxidizer–fuel–ratios are between 0.7 and 3.0 (V100 to V105). Due to the maximum mass flow limitations, pictured in Fig. 2, the OFR is not kept constant in this case and evaluation is done at 8 s, since the higher load conditions do not allow for longer run times. The resulting fluctuation amplitude increases strongly with the mean pressure level up to $\pm$8.9%. But, since the relative RMS values, specifying the energy content of the fluctuations, are still between 1.4% to 4.3% and the peak distribution is random, the combustion is rough but stable. Again, the spectral distribution does not show a clear trend with increasing mass flow rate. While different clusters of peaks appear for the different tests, it seems that in the range of 250 to 350 Hz, most tests show stronger oscillations. An exception is evident for V105, where the main content is located around 450 Hz. The shown data gives rise to the assumption, that further increasing the mass flow rate and oxidizer–fuel–ratio will lead to combustion instability.

3.4. *Injector Modification*

Since the future wind tunnel tests should rely on well-known input conditions to enable isolation of important flow features from disturbing influences at rough combustion, unnecessary fluctuations in the combustion chamber should be minimized. Therefore, a new injector geometry (I04) with a larger velocity ratio v_{H2}/v_{O2} by a factor of three was designed to improve the mixing processes and, therefore, improving combustion of the C01 test case, where the original injector geometry (I02) is far off design. The two injector geometries are compared at identical test conditions near C01 in Fig. 14 by providing a series of time-sequenced pressure frequency–amplitude diagrams. They are taken at an interval of 1.0 s for the first 15 s of the run.

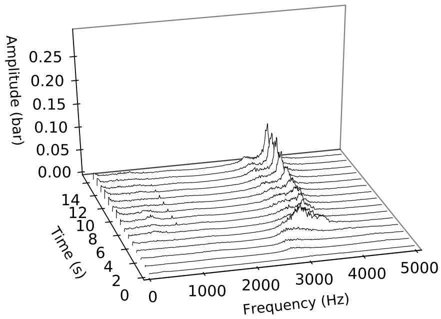

(a) Injector: I02, condition: RC0

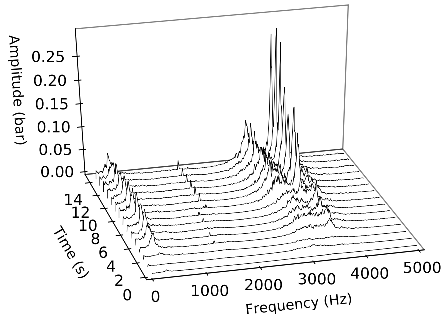

(b) Injector: I02, condition: C01

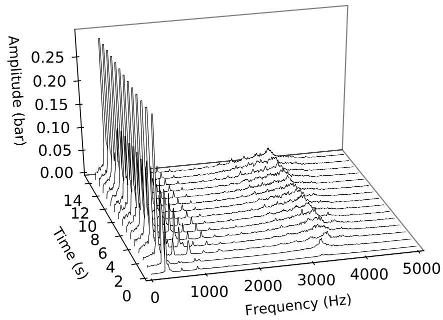

(c) Injector: I04, condition: C01

FIGURE 14. Spectogramm series of the chamber pressure signal at different conditions and injector geometries for the first 15 s of the run, taken every second

Figure 14(a), is used as a reference for the smooth combustion test case V139, which is comparable to the runs V128 and V100 at RC0 (Fig. 10 and Fig. 12). In addition to the negligible low frequency content, a screeching tone at about 3,450 Hz is detected. Considering the length of the chamber of approximately 255 mm in the middle of the converging nozzle part, and the speed of sound of approximately 1,750 m/s from one dimensional analysis, the detected frequency complies with the first natural longitudinal mode (L1) of the combustion chamber.† Figure 14(b) shows a run at increased oxidizer–fuel–ratio (V145), which is comparable to V132 (Fig. 10) and close to the C01 condition with $\pm$11.1% of relative peak to peak fluctuation. The present diagram shows a strong attenuation of the L1 mode and the broadband content at less than 500 Hz as observed above. After modifying the injector geometry, the same combustor input yields an unstable behavior with a very distinct oscillation at 250 Hz (Fig. 14(c)). The natural resonance frequency of the chamber is suppressed in this case, so that the RMS fluctuations of 14.3% are mainly contributed by this chugging frequency with a relative peak to peak amplitude of $\pm$26%, which corresponds to an oscillating pressure load of more than 10 bar.

† Notably, the first tangential mode (T1) of 13.5 kHz and the first radial mode (R1) of 42 kHz are not resolved by the pressure measurements.

	run#	t_{eval} / s	p_{cc} / bar	$\frac{p_{cc}'_{RMS}}{p_{cc}}$	$\frac{p_{cc}'_{pp}}{2 \cdot p_{cc}}$	injector	combustion state
baseline (RC0)	V137	30,0	22,23	1,03%	2,92%	I02	smooth
	V139	30,0	22,13	1,19%	4,27%	I02	smooth
	V141	30,0	22,21	1,21%	4,62%	I02	smooth
OFR variation	V128	15,0	21,21	1,20%	4,31%	I02	smooth
	V129	15,0	21,51	0,87%	3,12%	I02	smooth
	V130	15,0	23,95	1,14%	3,54%	I02	smooth
	V131	15,0	20,89	1,61%	5,10%	I02	rough
	V132	15,0	19,97	3,61%	8,85%	I02	rough
pressure variation	V100	8,0	17,80	1,44%	3,45%	I02	smooth
	V101	8,0	35,67	1,96%	4,79%	I02	smooth
	V102	8,0	44,24	3,34%	7,51%	I02	rough
	V104	8,0	51,27	3,86%	10,21%	I02	rough
	V105	8,0	58,97	4,29%	11,78%	I02	rough
injector variation (C01)	V132	15,0	19,97	3,61%	8,85%	I02	rough
	V145	15,0	21,56	4,08%	11,10%	I02	rough
	V134	15,0	19,72	14,17%	24,80%	I04	unstable
	V143	15,0	20,02	14,29%	25,99%	I04	unstable

TABLE 2. Summary of the test evaluation

4. Discussion and Outlook

Conceptually, the GH2/GO2 supply system including the combustor is regarded as a black box, that will provide input for high fidelity aerodynamic and aerothermodynamic measurements. The present work was conducted to characterize this system in order to demonstrate the suitability of the concept for future wind tunnel experiments in the scope of the SFB TRR40. This should be done for rather general variations of the supply system, but also for more specific requirements of the upcoming test configurations, namely the reference configurations RC0 and C01. For this reason, a test program was designed to investigate, the characteristics of the reference configuration RC0, and to expand the operating conditions towards C01, hence generating a suitable operating range.

4.1. *Qualification for Wind Tunnel Testing at RC0*

The input gas flows to the combustion chamber were investigated by observing the spectral content of the raw signals, the accuracy of their mean values, and the quality of the control behavior. The spectral content is interpreted as a realistic representation of an unsteady flow without significant deterministic disturbances. The accuracy of the primarily controlled quantities is within $\pm 1\%$ for the oxygen mass flow and $\pm 3\%$ for the hydrogen mass flow. The set point values are reached within these error bands within 7 s, providing long time constant and accurate operating conditions as input for the combustion chamber.

Repeatability is demonstrated for the resulting total chamber pressure and chamber wall temperature profiles, at reference configuration RC0. This holds for the final stationary conditions with a variation coefficient of 0.2% after 30 s runtime, as well as for the transient start-up process with an increasing variation to 1.3% after 5 s.

The combustion process at reference configuration RC0 is smooth within average relative peak-to-peak pressure amplitudes of $\pm$3.9% of the mean. The pressure fluctuations are mainly due to an occurring screeching frequency, which is identified as the first natural longitudinal mode (L1) at 3,450 Hz. The resulting wall temperature profiles are consistent and follow previous CFD calculations, except for a local temperature increase at 156 mm from the chamber base. We think that this phenomenon is linked to the L1 mode, which is coupling with an unsteady combustion process, causing small periodic detonations, that are locally disturbing the wall layers, formed by cold non-reacting hydrogen. This assessment is supported by a strong amplification of the phenomenon with increasing pressure amplitudes at higher operating conditions.

Provided, that the combustion process is smooth with reasonably low pressure fluctuations, its main impact is on the local heat flux, which is assumed not to be influencing the flow dynamics significantly.

4.2. *Qualification for Higher Operating Conditions*

With increased oxidizer–fuel–ratio towards C01, the response of the pressure fluctuation amplitude and the trend of the wall temperature anomaly are not yet satisfactory. For the current setup, an increase of OFR > 2.0 or an increase of the chamber pressure to approximately p_{cc} > 40 bar leads to a rough combustion state with $p'^{\text{p-p}}_{cc} > \pm 5\%$, increasing further with higher operating conditions.

For obtaining the C01 test case with smooth combustion, possible approaches would be to (1) limit the operating conditions to a maximum oxidizer–fuel–ratio of approximately 2.0 at a maximum chamber pressure of approximately 40 bar, (2) design a proper injector geometry with a favorable effect on the combustion dynamics to mitigate a further amplification of the natural frequencies of the chamber or fuel system, and (3) design proper acoustical absorbers for a damping of the L1 mode inside the combustion chamber.

The first attempt to improve combustion dynamics is a variation of the injector exit cross sections to alter the injection flow velocities. As a result, the L1 mode is attenuated significantly, whereas a massive instability is generated at a distinct frequency of 250 Hz with $p'^{\text{p-p}}_{cc} \approx \pm 26\%$. We assume that this strong amplification is due to a resonance between the altered injector flow dynamics and a structural mode of the flexible metallic tubing in the propellant supply lines. Further work for solving this issue is required.

Acknowledgments

Financial support has been provided by the German Research Foundation (Deutsche Forschungsgemeinschaft – DFG) in the framework of the Sonderforschungsbereich Transregio 40. The support of the technical staff during the work at the Supersonic and Hypersonic Technologies Department in Cologne is highly appreciated.

References

[1] ADAMS, N., STEMMER, C., RADESPIEL, R., SATTELMAYER, T., SCHRÖDER, W. AND WEIGAND, B. (2011). SFB-Transregio 40: Technologische Grundlagen für den Entwurf thermisch und mechanisch hochbelasteter Komponenten zukün-

ftiger Raumtransportsysteme – Motivation und Struktur. In: *60. Deutscher Luft- und Raumfahrtkongress*. Bremen, Germany.

[2] RADESPIEL, R., GLATZER, C., HANNEMANN, K., SAILE, D., SCHARNOWSKI, S., WINDTE, J., WOLF, C. AND YOU, Y. (2011). SFB-Transregio 40: Heckströmungen. In: *60. Deutscher Luft- und Raumfahrtkongress*. Bremen, Germany.

[3] DAVID, S. AND RADULOVIC, S. (2005). Prediction of Buffet Loads on the Ariane 5 Afterbody. In: *6th Symposium on Launcher Technologies*. Munich, Germany.

[4] DECK, S. AND THORIGNY, P. (2007). Unsteadiness of an Axisymmetric Separating-Reattaching Flow: Numerical Investigation. *Physics of Fluids*, **19**(065103), 1–20.

[5] STEPHAN, S. AND RADESPIEL, R. (2017). Propulsive jet simulation with air and helium in launcher wake flows. *CEAS Space Journal*, **9**(2), 195–209.

[6] SCHREYER, A.M., STEPHAN, S. AND RADESPIEL, R. (2017). Characterization of the supersonic wake of a generic space launcher. *CEAS Space Journal*, **9**(1), 97–110.

[7] STATNIKOV, V., BOLGAR, I., SCHARNOWSKI, S., MEINKE, M., KÄHLER, C. AND SCHRÖDER, W. (2016). Analysis of characteristic wake flow modes on a generic transonic backward-facing step configuration. *European Journal of Mechanics - B/Fluids*, **59**, 124–134.

[8] SAILE, D., KIRCHHECK, D., GÜLHAN, A. AND BANUTI, D. (2015). Design of a Hot Plume Interaction Facility at DLR Cologne. In: *Proceedings of the 8th European Symposium on Aerothermodynamics for Space Vehicles*. Lisbon, Portugal.

[9] (2016). GH2/GO2 Supply Facility for Hot Plume Testing in the Vertical Test Section Cologne (VMK). In: *Sonderforschungsbereich/Transregio 40 – Annual Report 2016*.

[10] SAILE, D., KIRCHHECK, D., GÜLHAN, A., SERHAN, C. AND HANNEMANN, V. (2015). Design of a GH2/GOX Combustion Chamber for the Hot Plume Interaction Experiments at DLR Cologne. In: *Proceedings of the 8th European Symposium on Aerothermodynamics for Space Vehicles*. Lisbon, Portugal.

[11] KIRCHHECK, D. AND GÜLHAN, A. (2017). Launch of the GH2/GO2 Supply Facility for Hot Plume Testing at DLR Cologne. In: *Sonderforschungsbereich/Transregio 40 – Annual Report 2017*.

[12] MARSHALL, W.M., PAL, S., WOODWARD, R.D. AND SANTORO, R.J. (2005). Benchmark Wall Heat Flux Data for a GO2/GH2 Single Element Combustor. In: *41st AIAA/ASME/SAE/ASEE Joint Propulsion Conference & Exhibit*. Tucson, Arizona.

[13] SUTTON, GEORGE, P. AND BIBLARZ, O. (2001). *Rocket Propulsion Elements*. John Wiley & Sons.

[14] HARRJE, DAVID, T. (Ed.) (1972). *Liquid Propellant Rocket Combustion Instabilities*. National Aeronautics and Space Administration (NASA).